

Supporting Information

Organ-restricted vascular delivery of nanoparticles for lung cancer therapy

Deniz A. Bölükbas, Stefan Datz, Charlotte Meyer-Schwickerath, Carmela Morrone, Ali Doryab, Dorothee Gößl, Malamati Vreka, Lin Yang, Christian Argyo, Sabine H. van Rijt, Michael Lindner, Oliver Eickelberg, Tobias Stoeger, Otmar Schmid, Sandra Lindstedt, Georgios T. Stathopoulos, Thomas Bein, and Darcy E. Wagner, Silke Meiners**

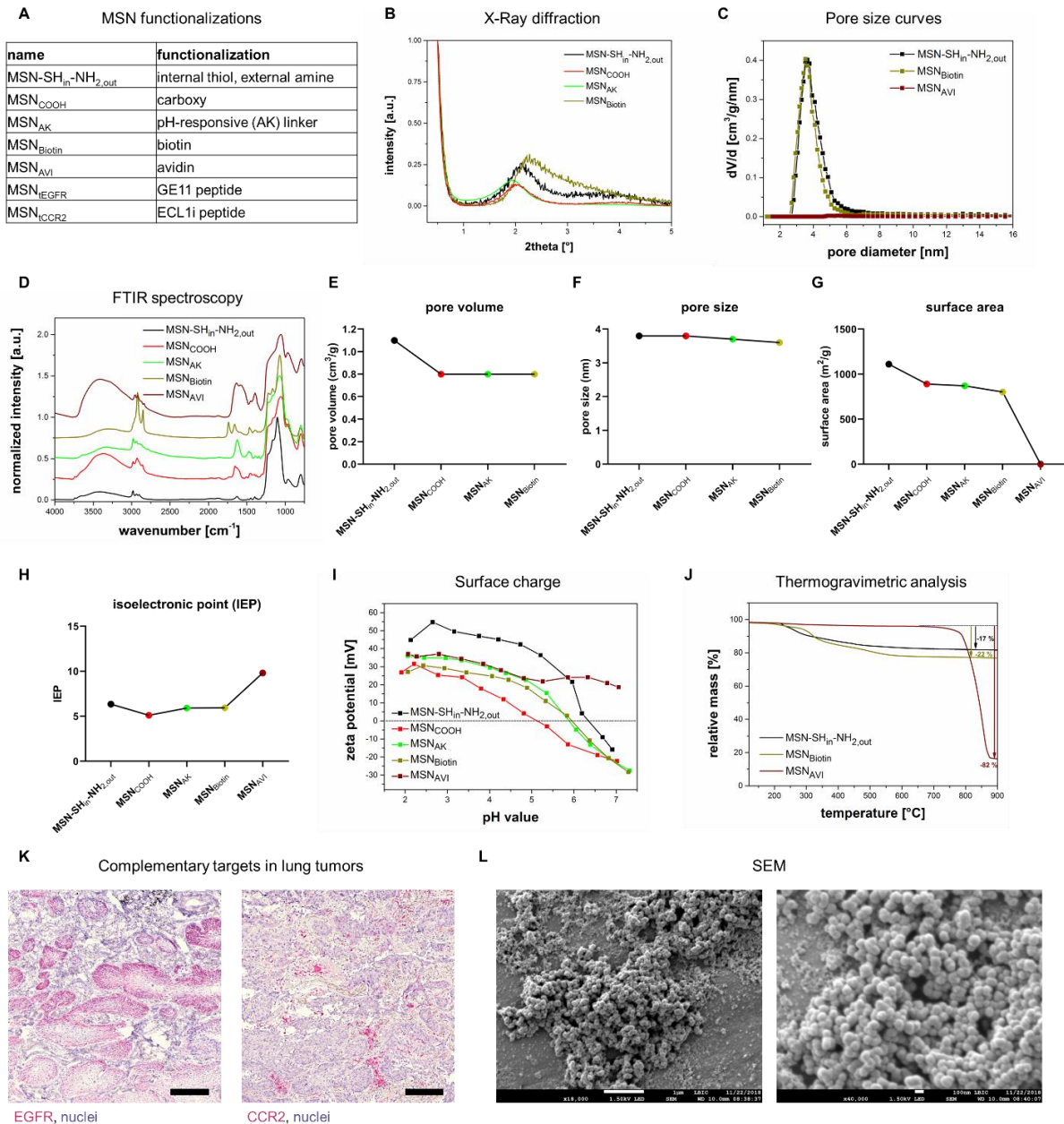


Figure S1. Physicochemical characterization of the MSNs. a) Summary of MSN functionalizations used. b) Small-angle X-ray scattering showing amorphous properties, c) pore diameter distribution curves, d) infrared spectroscopy, e) pore volume, f) pore size, g) surface area, h) isoelectric point (IEP), i) zeta potential measurements, j) thermogravimetric analysis for the different functionalization stages. k) Immunohistochemical staining representing complementary distribution of EGFR and CCR2 in a human non-small cell lung cancer (NCSLC) specimen. Scale bar = 200 μm . l) Scanning electron microscopic images of MSN_{EGFR}. Scale bar = 1 μm (left) and 100 nm (right).

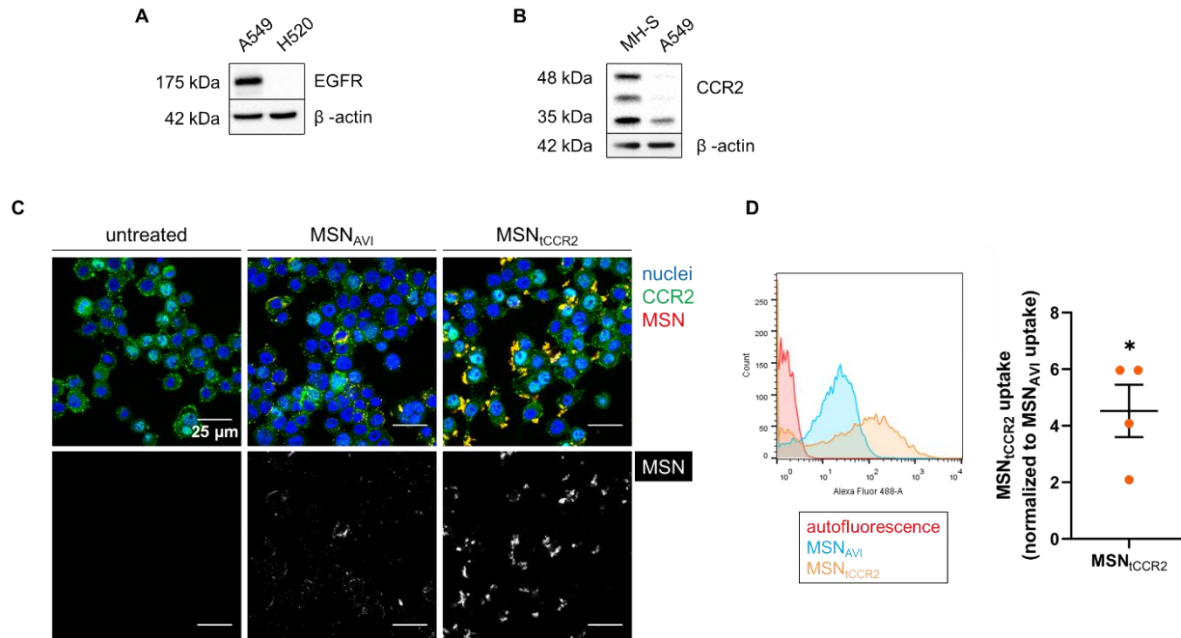


Figure S2. Increased uptake of CCR2 targeted nanoparticles in murine alveolar macrophages *in vitro*. a) EGFR expression in A549 cells in comparison to another NSCLC cell line, H520 cells, b) Western blot analysis of CCR2 expression in murine alveolar macrophage (MH-S) cells in comparison to A549 cells. c) Untargeted *versus* CCR2-targeted uptake of ATTO 633-labeled MSN_{AVI} and MSN_{ICCR2} (red in the upper panel, gray in the lower panel) by MH-S cells after 1 h; CCR2 (green) and cell nuclei (blue) visualized by confocal microscopy. Scale bar = 25 μ m. d) Increased uptake of ATTO 488-labeled MSN_{ICCR2} *versus* MSN_{AVI} after 1 h by MH-S cells measured by flow cytometry analysis. * $p = 0.0286$, Mann-Whitney test; values given are an average of four independent experiments \pm standard error of the mean.

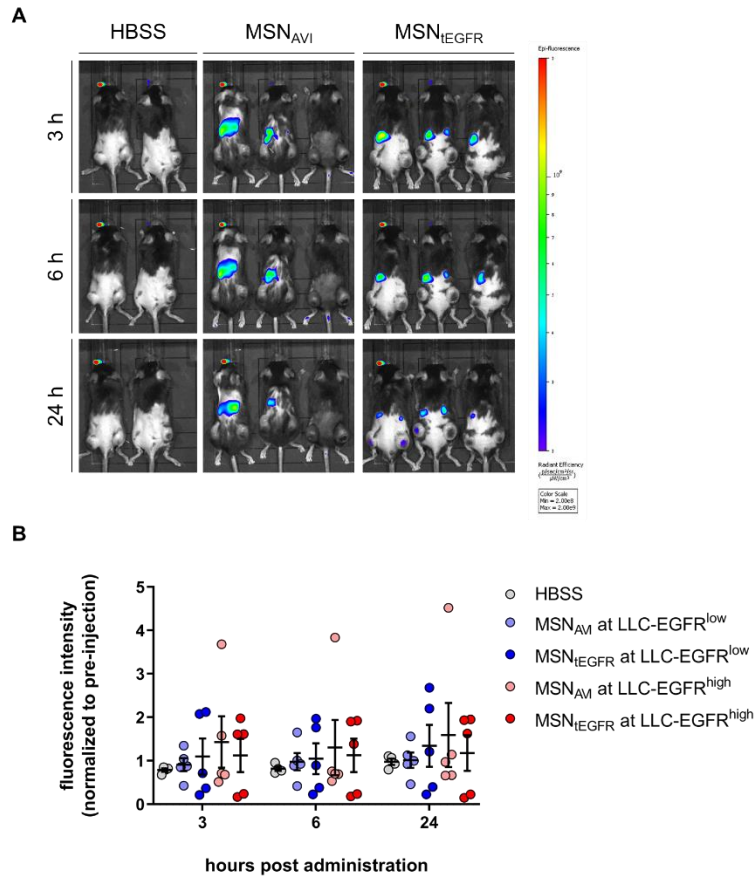
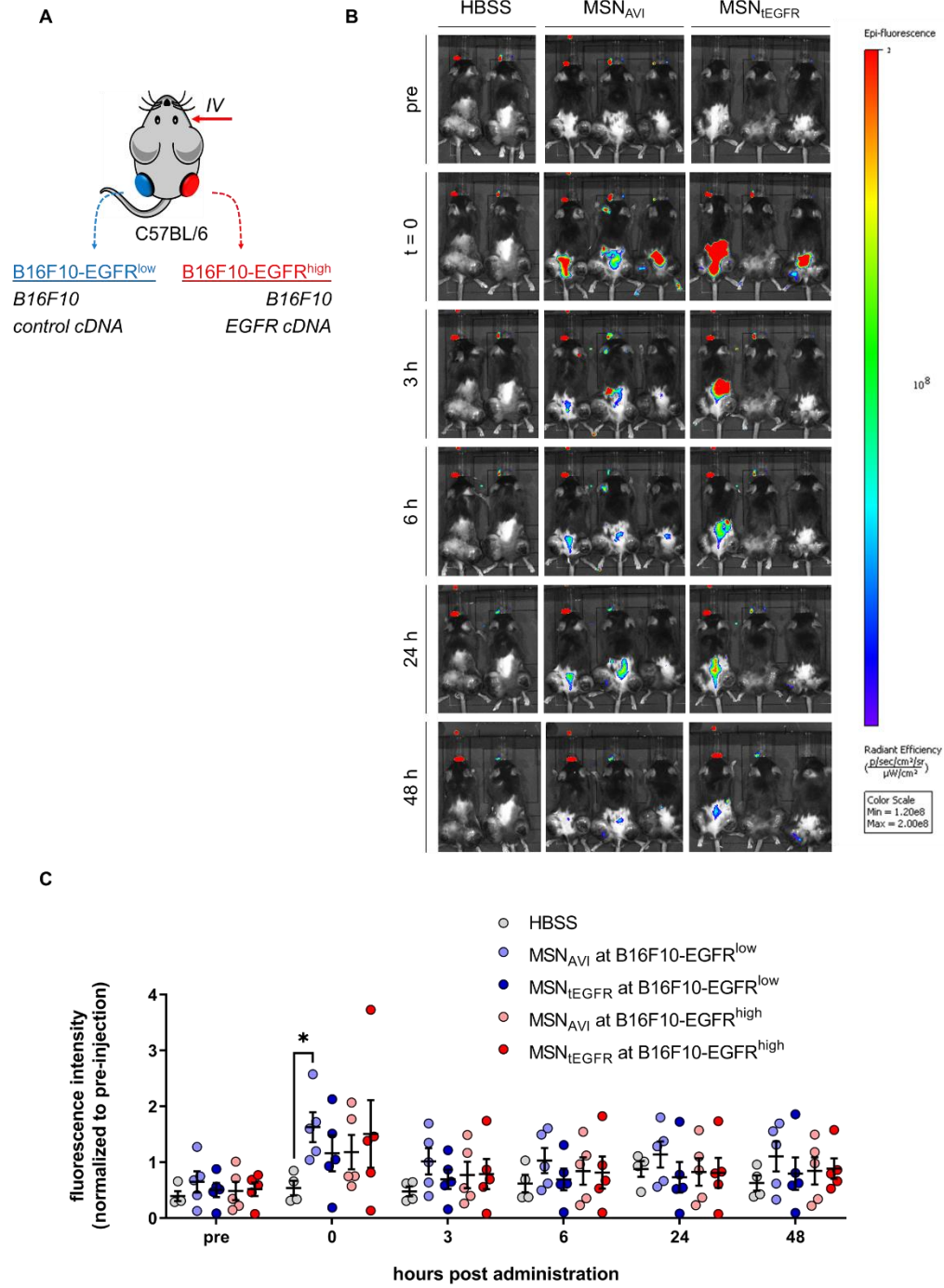
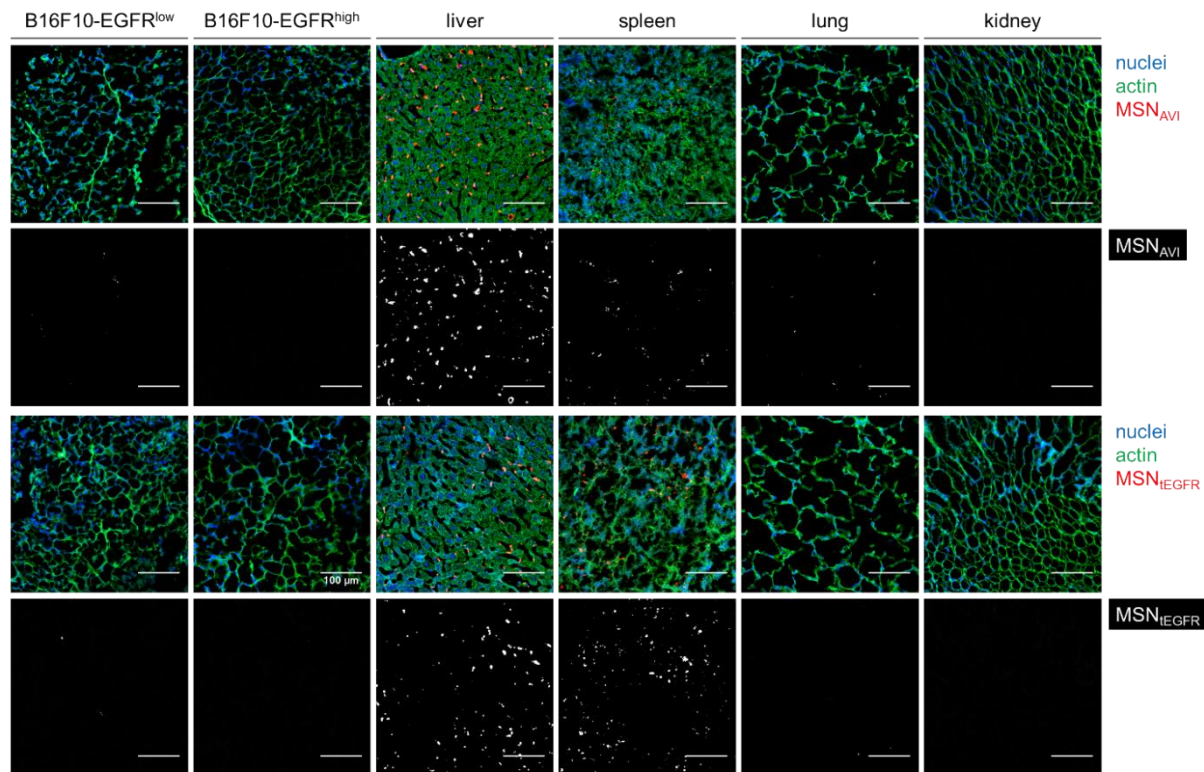


Figure S3. Intravenously administered MSNs are distributed unspecifically in a syngeneic LLC tumor model *in vivo*. a) Representative fluorescence images of mice receiving 1 mg of MSN_{AMI} or MSN_{IEGFR} at 3, 6, and 24 h after retro-orbital administration. b) Quantification of the fluorescence intensity obtained from the individual flank tumors of the mice treated with the MSNs in time course. Values given are an average of signal obtained from five independent mice at each time point \pm standard error of the mean ($n = 5$ mice per MSN type).



D



E

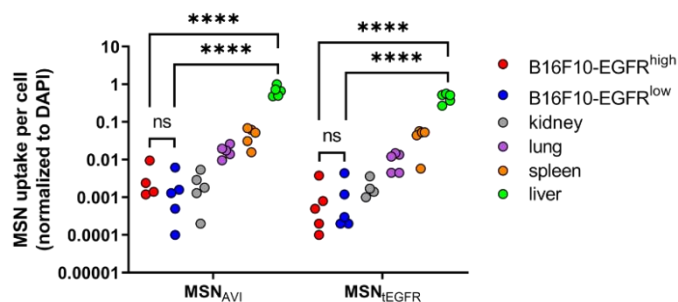


Figure S4. Intravenously administered MSNs are deposited in the liver and spleen in a syngeneic melanoma tumor model *in vivo*. a) Schematic representation of the syngeneic double flank tumor-bearing mouse model that was generated by subcutaneous injection of genetically modified melanoma clones (B16F10) for basal EGFR expression (B16F10-EGFR^{low}) versus overexpression (B16F10-EGFR^{high}). b) Representative fluorescence images of mice receiving 1 mg of MSN_{AVI} or MSN_{IEGFR} before, immediately after, or at 3, 6, 24, and 48 h after retro-orbital administration. c) Quantification of the fluorescence intensity obtained from the individual flank tumors of the mice treated with the MSNs in time course. Values given are an average of signal obtained from five independent mice at each time point \pm standard error of the mean. * $p = 0.0324$, Two-way ANOVA, Tukey's multiple comparisons test. d) Histological analysis for the biodistribution of the intravenously administered MSN_{AVI} and MSN_{IEGFR} in B16F10-EGFR^{low} and B16F10-EGFR^{high} tumors, livers, spleens, lungs, and kidneys of the mice visualized by

confocal microscopy. Nuclear staining (DAPI) is shown in blue, cell morphology via actin staining (phalloidin) in green and ATTO 633-labeled MSNs in red in the merged image, and in gray in the single channel. Images shown are representative for three different regions from each mice ($n = 5$ mice treated). Scale bar = 100 μm . e) Quantification of the MSN_{AVI} and $\text{MSN}_{\text{tEGFR}}$ uptake per nuclei observed in histological analyses in B16F10-EGFR^{low} and B16F10-EGFR^{high} tumors, kidneys, lungs, spleens, and livers, respectively. In the HBSS control, animals only received HBSS and no particles. Values given are average of three different images per each treated mice \pm standard error of the mean ($n = 5$ per MSN type). **** $p < 0.0001$, Two-way ANOVA, Tukey's multiple comparisons test.

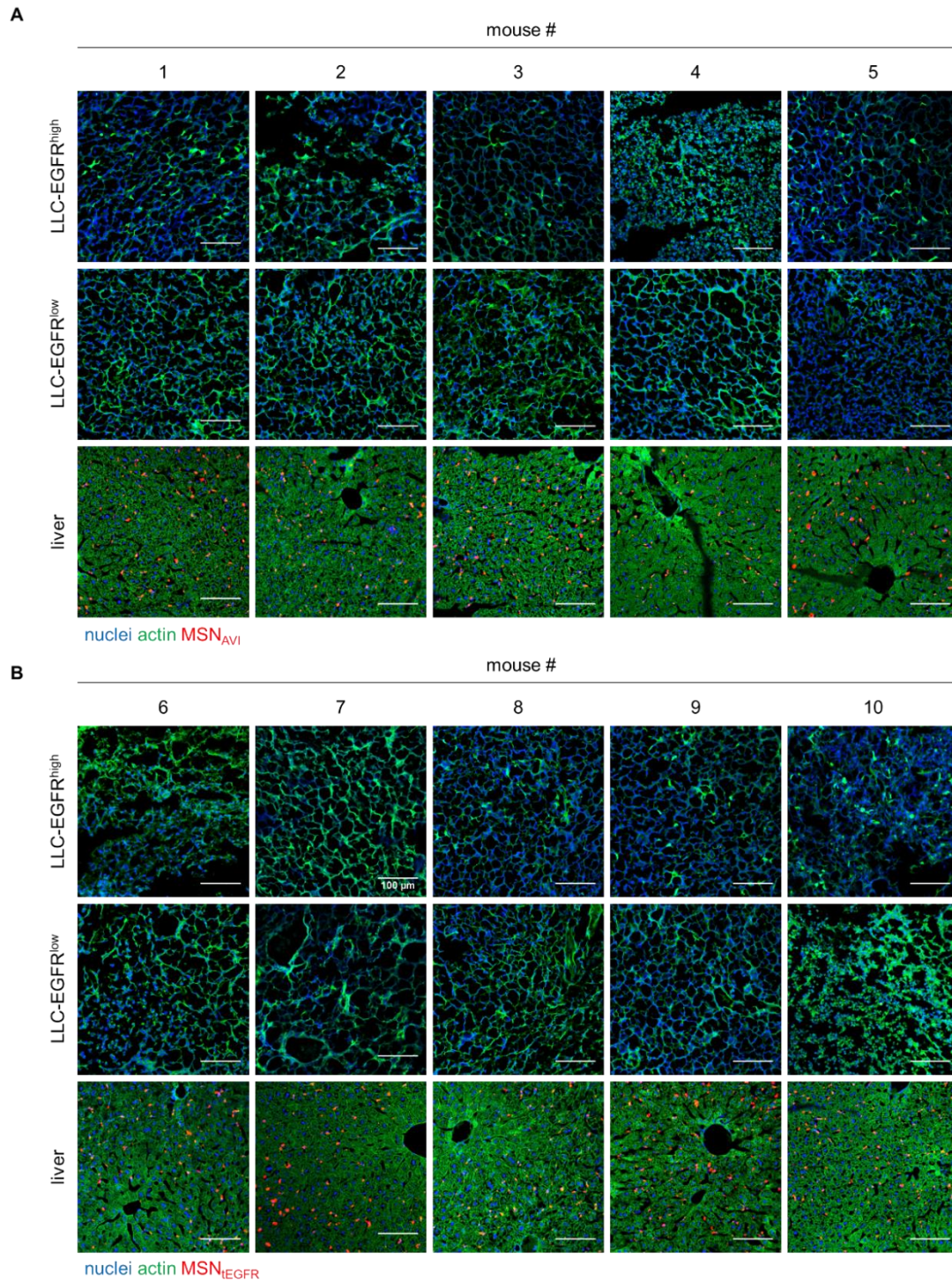


Figure S5. Intravenously administered MSNs are deposited to liver in a syngeneic LLC tumor model *in vivo*. Histological analysis for the biodistribution of the retro-orbitally administered a) MSN_{AVI} and b) MSN_{EGFR} in the LLC-EGFR^{high} tumors, LLC-EGFR^{low} tumors, and livers of each treated mice by confocal microscopy. Nuclear staining (DAPI) is shown in blue, cell morphology via actin staining (phalloidin) in green, and ATTO 633-labeled MSNs in red.

Images shown are representative for three different regions from each mice (n = 5 mice per MSN type). Scale bar = 100 μ m.

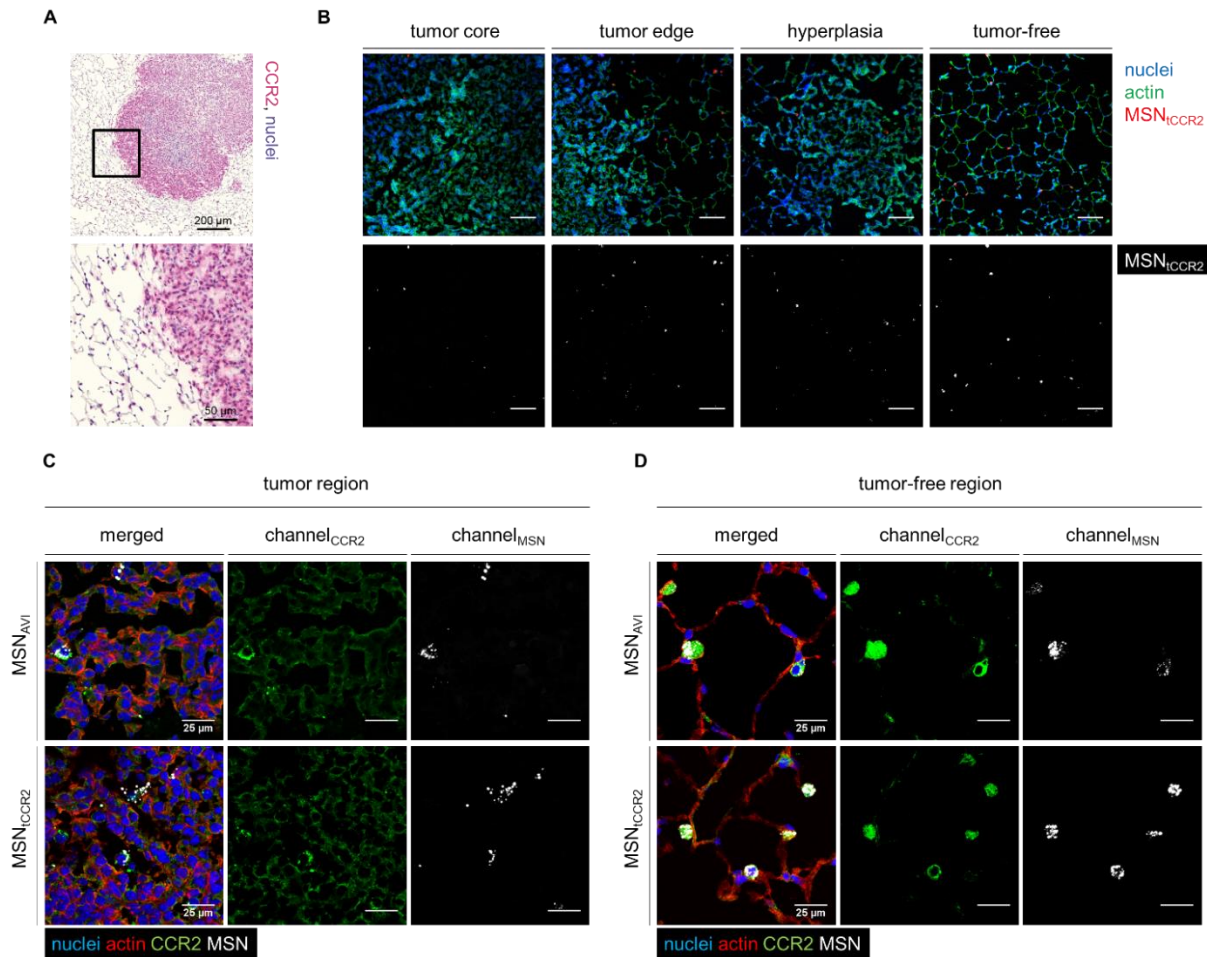


Figure S6. Intratracheally administered MSN_{CCR2} are engulfed by alveolar macrophages in a mouse model of lung cancer *in vivo*. a) Immunohistochemistry staining of CCR2 (pink) in *Kras*^{LA2} mutant tumorous mouse lungs. b) Representative histological analysis of intratracheally instilled ATTO 633-labeled MSN_{CCR2} uptake in solid tumor cores *versus* their edges, and in hyperplastic or in tumor-free regions of the tumorous mouse lungs, after 3 days. Nuclear staining (DAPI) is shown in blue, cell morphology via actin staining (phalloidin) in green, and ATTO 633-labeled MSNs in red in the merged images, and in gray in the single channels. Five mice were analyzed per group with five random sections and three images per section in a blinded manner. Images shown are representative for three different regions from each group of mice (n = 5 per MSN type). Scale bar = 100 μm . Immunofluorescence co-staining for CCR2 in c) tumorous *versus* d) tumor-free regions the mutant lungs treated with ATTO 633-labeled MSN_{AVI} *versus* MSN_{CCR2}. Nuclear staining (DAPI) is shown in blue, cell morphology via actin staining (phalloidin) in red, CCR2 staining in green, and ATTO 633-labeled MSNs in gray. Images shown are representative for three different regions from each group of mice (n = 5 per MSN type). Scale bar = 25 μm .

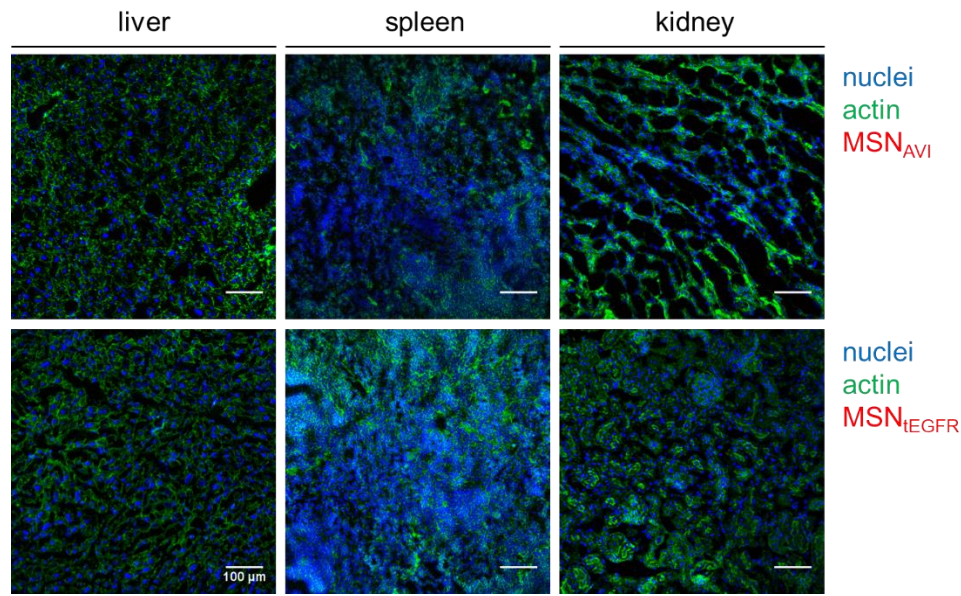


Figure S7. MSN_{AVI} and MSN_{IEGFR} do not localize to the liver, spleen or kidney when administered intratracheally into *Kras*^{LA2} mutant mice. Representative histological analysis of intratracheally administered ATTO 633-labeled MSN_{AVI} and MSN_{IEGFR} are not present in livers, spleens, and kidneys of the *Kras*^{LA2} mutant mice 3 days. Nuclear staining (DAPI) is shown in blue, cell morphology via actin staining (phalloidin) in green, and ATTO 633-labeled MSNs in red. Images shown are representative for three different regions from each mice (n = 5 per MSN type). Scale bar = 100 μm.

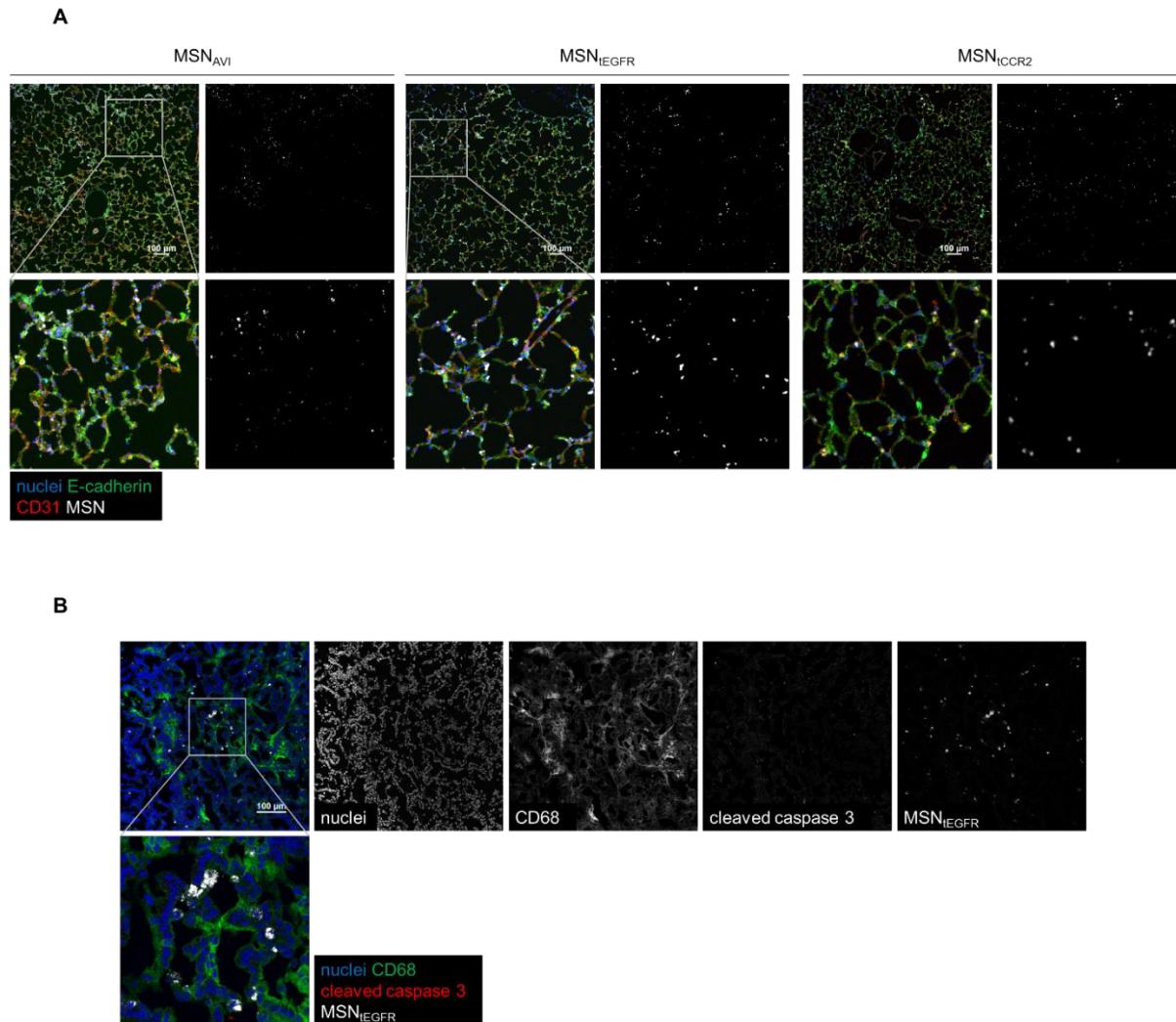


Figure S8. Organ-restricted vascular delivery of MSNs. a) Representative histological analysis of the lungs from WT mice exposed to ATTO 633-labeled MSN_{AVI} , MSN_{IEGFR} , and MSN_{ICCR2} (all gray). Nuclei were stained with DAPI (blue), epithelial cells labeled with E-Cadherin (green) and endothelial cells labeled with CD31 (red) shown in merged and corresponding single channel images for the nanoparticles. Scale bar = 100 μ m. b) Histological analysis of the solid tumors from the $Kras^{LA2}$ mutant lungs exposed to ATTO 633-labeled MSN_{IEGFR} (gray). Nuclei were stained with DAPI (blue), monocytes/macrophages labeled with CD68 (green) and apoptotic cells labeled with cleaved caspase-3 (red) shown in merged and corresponding single channel images. Scale bar = 100 μ m.